Food and Bioprocess Technology (2021) 14:751–764
https://doi.org/10.1007/s11947-021-02602-5

ORIGINAL RESEARCH

Valorization of Native Soluble and Insoluble Oat Side Streams for Stable Suspensions and Emulsions

Fabio Valoppi[1,2] · Yu-Jie Wang[1,3] · Giulia Alt[1,4] · Leena J. Peltonen[5] · Kirsi S. Mikkonen[1,2]

Received: 3 August 2020 / Accepted: 2 February 2021 / Published online: 11 February 2021

Abstract

Among different cereals, oat is becoming more popular due to its unique composition and health benefits. The increase in oat production is associated with an increase in related side streams, comprising unutilized biomass that is rich in valuable components, such as polysaccharides, proteins, and antioxidants. To valorize such biomass, it is fundamental that side streams enter back into the food production chain, in respect of the circular economy model. Here, we propose the use of soluble and insoluble oat-production side-stream in suspensions and emulsions, avoiding any further extraction, fractionation, and/or chemical derivatization. Our approach further increases the value of these side streams. To this aim, we first studied the effect of thermal and mechanical processes on the behavior and properties of both soluble and insoluble oat side-stream fractions in water and at air/water interface. Then, we characterized the emulsifying and stabilizing abilities of these materials in oil-in-water emulsions. Interestingly, we found that the insoluble fraction was able to form stable suspensions and emulsions after mechanical treatment. The oil droplets in the emulsions were stabilized by anchoring at the surface of the insoluble particles. On the other hand, the soluble fraction formed only stable viscous solutions. Finally, we demonstrated that the two fractions can be combined to increase the storage stability of the resulting emulsion.

Our results highlight that oat production side streams can be used as novel bio-based emulsifiers, showing the great potential behind the underutilized cereal-side-stream biomass.

Keywords Oat · Side stream materials · Emulsion · Stability · Beta-glucan · Arabinoxylan

Introduction

The cereal industry is the leading primary accounting for around 60% of the total world food production (Anal 2017). Oat (Avena sativa L.) has recently attracted the attention of both consumers and the scientific community due to its unique composition, including many nutrients required for maintaining health and reducing the risk of degenerative disease incidence (Gangopadhyay et al. 2015; Stewart and McDougall 2014). Oat production ranks sixth in the world cereal production statistics, following wheat, maize, rice, barley, and sorghum. Furthermore, contrary to other crops, oat can also be cultivated in harsh climate conditions such as those present in Northern Europe and Canada (Ahmad et al. 2014).

Due to the large production volumes, the cereal industry generates an important source of side streams such as husks, hulls, and bran (Anal 2017). Bran is the main by-product obtained from cereal milling, with, e.g., 90 million tons of wheat bran produced annually worldwide (Onipe et al. 2015). The side streams are commonly used for feed,

Fabio Valoppi and Yu-Jie Wang contributed equally to this work.

✉ Kirsi S. Mikkonen
kirsi.s.mikkonen@helsinki.fi

[1] Department of Food and Nutrition, University of Helsinki, P.O. Box 66, (Agnes Sjöbergin katu 2), FI-00014 Helsinki, Finland

[2] Helsinki Institute of Sustainability Science, Faculty of Agriculture and Forestry, University of Helsinki, FI-00014 Helsinki, Finland

[3] Present address: Department of Chemistry, Institute of Material Sciences, Nestlé Research, Route du Jorat 57, 1000 Lausanne, CH, Switzerland

[4] Present address: Washing Technology, Division: Chemical Technology, Electrolux Italy S.p.A., Corso Lino Zanussi, 24, 33080 Porcia, PN, Italy

[5] Division of Pharmaceutical Chemistry and Technology, Drug Research Program, University of Helsinki, P.O. Box 56, (Viikinkaari 5 E), FI-00014 Helsinki, Finland

fertilization, and energy production through, e.g., gasification and pyrolysis (Arvanitoyannis and Tserkezou 2008). However, they also provide a large quantity of unutilized biomass rich in valuable components, such as polysaccharides, proteins, and antioxidants (Helkar et al. 2016; Luithui et al. 2019). Bran is rich in arabinoxylan, polyphenols, phytosterols, and β-glucan. β-glucan is an indigestible unbranched polysaccharide consisting of β-D-glucose units linked through (1→4) and (1→3) glycosidic bonds (Charalampopoulos et al. 2002; Papageorgiou et al. 2005). It is mainly found in endosperm cell walls and in the internal aleurone (Charalampopoulos et al. 2002). Oat and barley have the highest concentration of β-glucan in bran, ranging between 6.5 and 9.1% (Bhatty 1993; Luhaloo et al. 1998). Arabinoxylans are indigestible polysaccharides composed of a β-(1→4) xylopyranosyl backbone branched with α-arabinofuranosyl units at their O-2 and/or O-3 positions (Lv et al. 2019). In wheat and rye, arabinoxylans can make up to 22–30% of the bran (Kamal-Eldin et al. 2009; Maes and Delcour 2002), while oat bran contains around 2–5% arabinoxylan (Luhaloo et al. 1998). In addition, hydroxycinnamic acids, such as ferulic acid, are bound to the arabinosyl residue in arabinoxylans via an ester bond (Lv et al. 2019). Bran also contains vitamins, proteins, minerals, phytic acid, and saponins (Onipe et al. 2015; Ralla et al. 2018; Stevenson et al. 2012).

The cereal side-streams can be used for the development of bio-based materials and ingredients for functional foods (Sharma et al. 2016). For instance, cellulose nanofibers as reinforcing agents in packaging bio-composite materials have been successfully obtained from wheat straws, soy hulls, and rice husks (Fritsch et al. 2017). Bioplastics obtained from precursors extracted from cereal side-streams have been developed (Isikgor and Becer 2015), and cereal bran has been identified as a potential ingredient to obtain functional foods (Patel 2015). Many of the cereal phytochemicals have shown anti-inflammatory and anti-microbial effects, blood cholesterol, and glycemic response lowering ability, and intestinal health improvement effect (Izydorczyk et al. 2014; Luithui et al. 2019; Saeed et al. 2014). Due to its composition, bran from wheat and rye has been used as starting material to obtain additives and concentrates for functional food production such as carbohydrate-protein concentrate, dietary fiber, polyphenols, and prebiotic xylo-oligosaccharides (Kapreliants and Zhurlova 2017). Oat bran components such as β-glucan have been proved to reduce lipid digestibility in model emulsion systems which can be used to modulate digestion in functional foods (Grundy et al. 2018). Moreover, the antioxidant fraction of wheat and oat bran can also be increased using solid-state yeast fermentation leading to an enriched bran useful for functional food production (Călinoiu et al. 2019). In addition, as a heterogeneous material, bran has been used for extracting bio-based emulsifiers. For instance, rice bran proteins and partially hydrolyzed rice bran proteins have been successfully employed to stabilize oil-in-water emulsions (Sun et al. 2019; Zang et al. 2019). Oat bran extract has also been identified as a novel source of emulsifiers, such as saponins that are naturally occurring small molecular weight surfactants (Ralla et al. 2018). This peculiar composition makes oat transformation by-products a potential target for obtaining new bio-emulsifiers.

Proteins and saponins are known to have emulsifying ability due to their chemical composition and molecular geometry. Less is known regarding the emulsifying abilities of the other fractions present in cereal side-streams, such as hemicelluloses and polyphenols (β-glucan, arabinoxylan, lignin, etc.). Lv et al. (2019) covalently crosslinked wheat-bran arabinoxylan with whey-protein isolate using Maillard reaction, obtaining emulsifiers with good stabilization ability. However, the emulsifying capacity of native hemicelluloses or hemicellulose-bounded polyphenols present in cereal by-products has not yet been exploited. Our group recently demonstrated that softwood and hardwood extracts from sawdust can be employed for oil-in-water emulsion formation, stabilization, and protection against oxidation (Bhattarai et al. 2019; Lahtinen et al. 2019; Lehtonen et al. 2016, 2018; Mikkonen et al. 2016a). The extracts are a complex mixture containing hemicelluloses such as galactoglucomannans or glucuronoxylans (depending on the source), free and hemicellulose-bound phenolics, and residual lignin (Lahtinen et al. 2019; Lehtonen et al. 2018). Lignin and phenolic residues attached to hemicelluloses have been identified as being responsible for the emulsifying properties of the extracts (Lahtinen et al. 2019; Valoppi et al. 2019a). Due to the similarity in chemical species present in cereal bran and wood, we expect that by-products from the cereal-transformation industry can be employed as bio-based emulsifiers.

In this work, we studied the functional properties of side streams from oat transformation to form and stabilize oil-in-water emulsions. The heterogeneous starting material contained hemicelluloses such as β-glucan and arabinoxylans, phenolic compounds, and proteins that can be used to stabilize the oil/water interface and form emulsions. As such, we considered soluble and insoluble fractions extracted from oat production by-products. After characterizing the starting materials, we studied the effect of processing conditions such as temperature, time, and shear forces, on the behavior and properties in water and at air/water interface of the different fractions. Finally, we studied the emulsifying ability of sole and blended fractions, and we determined the stability of the resulting oil-in-water emulsions. The results highlighted that oat-transformation side-streams can be used as novel bio-based emulsifiers with no further fractionation and/or chemical derivatization, showing the great potential behind the underutilized hemicellulose-rich cereal side-streams.

Materials and Methods

Materials

The soluble (SOF) and insoluble (IOF) fractions obtained from oat transformation production were kindly donated by Lantmännen (Stockholm, Sweden) that also provided the chemical composition of the samples (Table 1). The starting material for producing IOF and SOF was a milled, air classified ethanol extracted dehulled oat kernel. The fraction used had a β-glucan content of 28%. IOF is the insoluble residue after water decanting for β-glucan extraction, and it mainly contains arabinoxylan, protein, and beta-glucan. IOF accounts for approximately 50% of the mass of the coarse fraction. SOF is the β-glucan-rich extract obtained after water extraction, precipitation with isopropanol, centrifugation, and washing with acetone, and it contains mainly β-glucan and proteins. SOF accounts for approximately 20% of the mass of the coarse fraction. Ethanol A 96.1% (v/v) was from Altia Oyj (Rajamäki, Finland). Sodium carbonate (Na_2CO_3) was purchased from Merck KGaA (Darmstadt, Germany), and citric acid monohydrate ($C_6H_8O_7 \cdot H_2O$) was purchased from Fisher Scientific UK (Leics, UK). Folin-Ciocalteu reagent was purchased from Merck KGaA (Darmstadt, Germany). Sodium azide (NaN_3), sodium nitrate ($NaNO_3$), disodium phosphate (Na_2HPO_4), monopotassium phosphate (KH_2PO_4), and sodium hydroxide (NaOH) were from Sigma Aldrich (Darmstadt, Germany). Gallic acid was from Extrasyntese (Genay, France). Rapeseed oil was purchased in a local supermarket. Calcofluor fluorescent stain was purchased from Megazyme (Wicklow, Ireland).

Table 1 Chemical composition of insoluble oat fraction (IOF) and soluble oat fraction (SOF)

Component (% dried matter)	Sample	
	IOF	SOF
Protein	21.8	11.1
β-glucan	20.8	77.5
Fat	4.6	0.0
Arabinoxylan	25.0	4.8
Cellulose	3.0	0.8
Ash	5.8	1.5
Starch	0.6	0.9
Maltodextrin	1.0	0.0

Note: protein content determined using elemental analysis of total nitrogen multiplied by 5.7; β-glucan content determined using AOAC 995.16 method; fat content determined according to Floch et al. (1957); arabinoxylan and cellulose content determined according to Englyst et al. (1994); ash content determined using AOAC 923.03 method; starch and maltodextrin contents determined using AOAC 996.11 method

Methods

Content of Phenolic Compounds and Phytic Acid

The analysis for the phenolic compounds was performed with the Folin-Ciocalteu method (Satue et al. 1995). Aliquots of 1% (w/v) IOF and SOF powders were dissolved in Milli-Q water at 80 °C for 2 h. Then, 150 μL of the sample was mixed with 750 μL of Folin-Ciocalteu reagent, and 600 μL of 7.5% (w/v) Na_2CO_3 was added. After vortexing, the test tubes were incubated in darkness at room temperature for 30 min. The absorbance of the sample was measured at 765 nm with a spectrophotometer (UV-visible spectrophotometer, UV-1800, Shimadzu, Japan). Water was used as blank. Total phenolic content was expressed as gallic acid equivalents (GAE) in mg/g of dry sample using a gallic-acid standard calibration curve.

The phytic acid content of the samples was measured as phosphorus released by phytase and alkaline phosphatase using a phytic acid kit from Megazyme.

Moisture Content

Around 100 mg of IOF and SOF was weighed in an aluminum container and dried in a vacuum oven (Vacucenter VC—20/50, Renggli AG, Salvis-Lab, Rotkreuz, Switzerland) at 50 °C for 72 h. Moisture content was calculated as a ratio between the weight of the water removed and the initial weight of the sample.

Fourier Transform Infrared Spectroscopy (FTIR)

Dried IOF and SOF (vacuum oven for 24 h at 50 °C) were analyzed using a Spectrum One Fourier transform infrared spectrometer (PerkinElmer, Waltham, MA, USA) mounted with a universal ATR sampling accessory. Spectra were acquired at 25 ± 1 °C using Spectrum v. 10 (PerkinElmer) application software. Samples were placed onto the Zn–Se crystal and pressed against the crystal using the ATR arm. Spectra were collected performing 10 scans for each sample between 4000 and 650 cm^{-1} with a resolution of 1 cm^{-1}. Background scan of the clean Zn–Se crystal was acquired prior to sample scanning.

Preparation of Aqueous Suspension and Emulsion

IOF and SOF (0.2, 0.5, 1.0, or 2.0 g) were first wetted with ethanol (sample to ethanol ratio of 1:40 w:v) in Erlenmeyer flasks before dispersion with 100 mL of Milli-Q water or 0.1 M sodium citrate-phosphate buffer at pH 4.5 or 7.0. The experiment was designed to study the impact of solubilization temperature and method/intensity of homogenization on the phase stability of the suspension. As such, the suspensions

were mixed at room temperature or 80 °C for 2 h. Some samples were homogenized by Ultra-Turrax (T-18 basic, IKA, Staufen, Germany) at 81620 × (22000 rpm) for 2 min and/or by microfluidizer 110Y (Microfluidics, Westwood, MA, USA) at 80 MPa for 4 passes. Selected samples were homogenized with microfluidizer twice.

The obtained suspensions (with or without homogenization) were then used for emulsion preparation. Rapeseed oil was added to the suspensions at different concentrations (0.5%, 1.0%, 2.5%, and 5.0% w/w), and the mixtures were first homogenized by Ultra-Turrax (UT) at 81620 × (22000 rpm) for 2 min to produce coarse emulsion and then homogenized with microfluidizer (MF) at 80 MPa for 4 passes to produce a fine emulsion.

After homogenization, all emulsions were added with 0.02% (w/v) sodium azide to prevent microbial spoilage during storage at 20 °C. Three replicates were made for each sample.

Water Solubility Index (WSI)

The water solubility index (WSI) was determined following the method from AOAC (1990) (El-Din et al. 2009). To study the effect of temperature and homogenization on the water solubility of IOF samples, 1% (w/v) IOF suspensions were mixed at room temperature for 2 h, heated at 80 °C for 2 h, homogenized by UT or MF before WSI determination. For SOF samples, only solubilization at room temperature and 80 °C for 2 h without homogenization was studied on 1% (w/v) suspension, because homogenization can degrade β-glucan molecules (Kivelä et al. 2010). After treatments, 30 mL of each sample was centrifuged with a Hermle Z323 centrifuge (Hermle Labortechnik GmbH, Wehingen, Germany) at 6000 × (3000 rpm) for 20 min. The supernatant was collected and dried with a vacuum oven at 50 °C for 24 h. The dried residue was weighed, and the WSI was calculated as the ratio (percentage) of the weight of the dried supernatant to the weight of the dry starting material.

Water Holding Capacity (WHC)

The effect of temperature and homogenization on water holding capacity (WHC) was studied using the centrifugation method described by Robertson and Eastwood (1981). After the treatments, 30 mL of 1% (w/v) IOF samples was centrifuged at 3000 rpm for 20 min, after which the excess water was decanted, and the tubes were inverted and left to drain for 10 min. The fresh weight of the sample was determined, and the WHC was calculated as the water retained by fiber divided by the dry weight of the starting material (g water/g fiber). Triplicates were performed.

Protein Solubility

Soluble protein content was determined using a Bio-Rad Protein Assay kit (Bio-Rad, Hercules, CA, USA) following the manufacturer's instructions and analyzing the samples at 595 nm with a UV-1800 UV-visible spectrophotometer (Shimadzu, Kyoto, Japan). A 5-point standard curve was obtained with bovine serum albumin.

Particle Size Measurement

The size distribution of the particles in suspension and oil droplets in emulsion, as well as the surface-weighted diameter D[3,2], volume-weighted diameter D[4,3], size distribution percentiles Dv(10), Dv(50), and Dv(90), and distribution width parameter SPAN (that is calculated as [Dv(90)–Dv(10)]/Dv(50)) were measured using a Mastersizer 3000 static light scattering apparatus mounted with a Hydro EV dispersion accessory (Malvern Instruments Ltd, Malvern, UK) controlled using the Mastersizer v.3.62 (Malvern Instruments Ltd.) application software. Before analysis, the suspensions and emulsions were gently turned upside down 10 times. The suspensions and emulsions were then diluted with deionized water directly into the dispersion accessory to avoid multiple scattering effects. The refractive indices of water, hemicelluloses, and oil were 1.33, 1.48, and 1.47, respectively. Triplicates were performed.

Morphology

Emulsions were analyzed using an optical microscope (AxioVision, Carl Zeiss, Microimaging GmbH, Jena, Germany) connected with an AxioCam MRm digital camera (Carl Zeiss, Microimaging GmbH, Jena, Germany). One drop of the upper part of the sample was placed in the middle of a glass slide, and a glass cover slip was centered above the drop. The samples were analyzed using a 100× objective. Images were acquired using AxioVision v.4.7.1.0 (Carl Zeiss, Inc., Germany) application software. For unstable emulsions, the creaming part of the emulsion was taken for observation. Before imaging, samples were mixed with 10 mg/L Calcofluor in 100 mM KH_2PO_4 at pH 10 (freshly prepared in the darkness) and observed under fluorescence. The excitation wavelength for Calcofluor was 365 nm, while the emission wavelength was 435 nm.

ζ-Potential

The ζ-potential of IOF and SOF samples after treatments (see Preparation of Aqueous Suspension and Emulsion paragraph) was determined using an electrophoretic light scattering instrument (Zetasizer Nano ZS series, Malvern Instruments Ltd, Malvern, UK). Before measurements, samples were

diluted to 0.5% using Milli-Q water or buffer to avoid multiple scattering effects. After loading the samples in the folded capillary cells and inserting into the instrument, they were equilibrated at 25 °C for 2 min. Next, three repeated measurements obtained from 30 continuous readings on each sample were recorded. ζ-Potential was calculated applying the Smoluchowski model on the acquired electrophoretic data using Dispersion Technology Software v. 5.10 (Malvern Instruments). Each measurement was repeated three times.

Surface Tension

The surface tension was measured with a du Nouy tensiometer (KSV Sigma 70, KSV, Finland) using a platinum ring. Surface tension was determined at room temperature measuring the maximum pull force of a platinum ring moving the solution outwards at a speed of 5 mm min^{-1}. The surface tension was measured on Milli Q water-based or buffer-based aqueous solutions containing 0.1% (w/w) of IOF and SOF solubilized at 80 °C for 2 h. As a reference, the surface tension of the sodium citrate-phosphate buffer and Milli-Q water was measured. Around 15 mL of each sample was poured into a cylindrical container and allowed to rest for 20 min before the measurement. Three different measurements for each sample were carried out at 5-min intervals in order to ensure a sufficiently long stabilization time.

Viscosity

The viscosity value of treated IOF and SOF suspensions, as well as their blends at different ratios, was measured using a rheometer (Haake Rheostress 600, Thermo Electron GmbH, Germany) with a cone and plate geometry (35 mm, 2°). The measurement was carried out with shear rate ranges from 10 s^{-1} to 100 s^{-1} at 20 °C. The viscosity value at a shear rate of 10 s^{-1} was used for comparison of samples. For unstable IOF suspension, the supernatant was taken for triplicate viscosity measurements.

Physical Stability

Suspensions (0.2%, 0.5%, and 1% w/w) and emulsions prepared with IOF and SOF were monitored by Turbiscan Lab Expert analyzer (Formulaction, Toulouse, France) and recorded by taking pictures during the storage for 5 weeks. Around 20 mL of sample was poured into glass transparent vials and kept at room temperature undisturbed. During measurement, the vials were vertically scanned from the bottom to the top by a near-infrared light (λ = 880 nm) source. Detectors simultaneously measured the intensity of transmitted and backscattered light at 180° and 45°, respectively. The Turbiscan stability index (TSI) was calculated with the Turbiscan software (v. 1.2) based on the changes in backscattering values during storage over sample height. An increase of TSI over time indicates a decrease of sample stability.

Data Analysis

All determinations were expressed as the mean ± standard deviation (SD) of at least two measurements from two experimental replicates ($n \geq 2 \times 2$), if not otherwise specified.

Statistical analysis was performed using R v. 3.5.1 (The R Foundation for Statistical Computing). Bartlett's test was used to check the homogeneity of variance, one-way ANOVA was carried out, and Tukey's-test was used as a post hoc test to determine significant differences among means ($p < 0.05$). Correlation analysis expressed by means of Pearson product-moment coefficient (r), hereafter, called Pearson correlation coefficient, was performed using Microsoft Excel Office 365 (Microsoft Corporation). The significance of Pearson correlation coefficients ($p < 0.05$) was tested using the t-test.

Turbiscan suspension stability data were fitted using TableCurve 2D (Jandel Scientific, ver. 5.01). Non-linear regression analysis was performed using (Eq. 1):

$$\mathrm{TSI} = \mathrm{TSI}_{\max} \cdot \left(1 - e^{-K \cdot t}\right) \quad (1)$$

where TSI is the Turbiscan stability index, $\mathrm{TSI}_{\max}$ is the maximum TSI reachable at infinite times, K is the rate constant, and t is time. The Levenberg-Marquardt algorithm was used to perform least-squares function minimization, and the goodness of fit was evaluated based on statistical parameters of fitting (R^2, p, and standard error) and the residual analysis.

Data were plotted using GraphPad Prism v. 5.03 (GraphPad Software, San Diego, CA, USA).

Results and Discussion

Characterization of Soluble and Insoluble Oat Fraction Powders

We first characterized the soluble (SOF) and insoluble (IOF) fractions extracted from oat. These fractions are heterogenous materials composed mainly of hemicelluloses such as β-glucan and arabinoxylan and proteins (Table 1). IOF was the most heterogeneous material with a ratio among β-glucan, arabinoxylan, and proteins of around 1:1:1, and with the presence of fat and ashes. The powder appeared brownish with a moisture content of 2.4%, containing 4.0 mg_{GAE}/g of phenolic compounds and 3.0% (dry matter basis) of phytic acid. On the other hand, SOF was more homogeneous showing a high share of β-glucan and a ratio among β-glucan, arabinoxylan, and proteins of 16:1:2.3. The material was a white fine powder with a moisture content of 6.0%, containing 1.1 mg_{GAE}/g of

phenolic compounds and 1.2% of phytic acid. IOF contains a higher amount of polyphenols and phytic acid compared to SOF. Oat bran is known to be higher in phenolic compounds than other oat fractions or products. The most abundant phenolic compound is ferulic acid (Soycan et al. 2019), which is commonly associated with arabinoxylan. IOF contained a higher content of arabinoxylan, which contributed to the higher polyphenolic compounds. In cereals, phytic acid is mainly located in the bran (protein globois), and it is insoluble in water at neutral or alkaline pH (Schlemmer et al. 2009), which explained the high amount of phytic acid in IOF. However, 1.2% of phytic acid was still found in SOF which was co-extracted and co-precipitated with beta-glucan when using organic solvent such as ethanol (Wang et al. 2020).

To gather more information on the functional groups present in SOF and IOF, we performed Fourier transform-infrared (FT-IR) spectroscopy (Fig. 1). The spectrum of both samples displayed similar peaks. Intense absorption bands were found for both samples at 1038–1066 cm^{-1}. These bands coupled to those at 1156 and 895 cm^{-1} can be attributed to the abundant β-glucans and arabinoxylans in both samples (Ahmad et al. 2010; Morales-Ortega et al. 2013; Synytsya and Novak 2014). Absorption bands at 1648–1642 cm^{-1} could be due to functional groups of proteins, such as C-N and N-H (Ahmad et al. 2010). We also found characteristic bands at 1380–1378 cm^{-1} and 1530 cm^{-1}, which can be related to the presence of phenols (O-H bending in phenolic molecules) and polyphenols (aromatic skeleton vibration), respectively (Faix 1991), revealing the presence of phenolic compounds in accordance with phenolic content data. The band at 1735 cm^{-1} was present only in the IOF sample, which can be attributed to the stretching of carboxylic ester groups (Song and Hubbe 2014), most probably due to the presence of triacylglycerols in the IOF sample (Table 1).

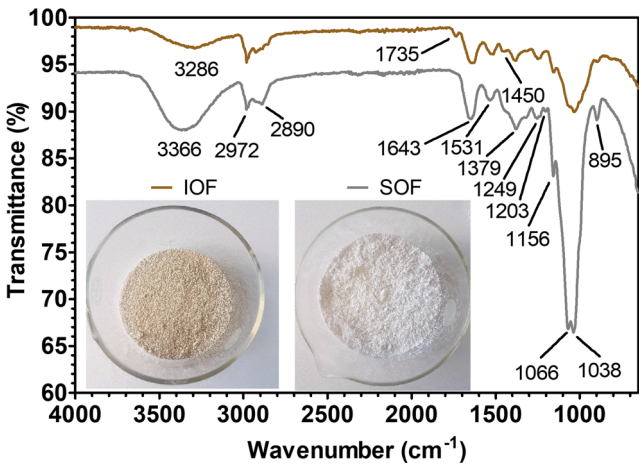

Fig. 1 FT-IR transmission spectra for insoluble (IOF, brown) and soluble (SOF, grey) oat fractions. Inset shows the macroscopic appearance of the two fractions (left: IOF, right: SOF)

Behavior and Physical Stability of Oat Fractions in Different Media and Under Different Treatments

Powders were then dispersed in water or buffer, and the effect of processing conditions such as thermal treatment, high-speed homogenization (Ultra Turrax, UT), and high-pressure homogenization (microfluidizer, MF) was studied on water solubility, water holding capacity, and protein solubility.

First, we determined the water solubility of both SOF and IOF at room temperature for 2h, which was less than 10% and used as a reference. A substantial improvement was achieved by heating the systems. SOF dissolved well (solubility > 90%) after heating at 80 °C for 2 h. With the same heating procedure, the solubility of IOF increased to 25%. We then tested shear forces on the solubility of IOF and SOF. After high-speed homogenization at room temperature, the solubility of IOF did not significantly increase compared to mixing at room temperature. However, high-pressure homogenization considerably increased the solubility of IOF, which was similar to the values obtained with the heat treatment (Fig. 2a). Regarding the water holding capacity of IOF, heat treatment and high-pressure homogenization were able to increase it from 8 to 10 and 12 g_{H2O}/g_{IOF}, respectively. Fibers with high water-holding capacity are known to promote gut health (Yamazaki et al. 2005). On the other hand, high-speed homogenization reduced the water holding capacity of IOF to 6 g_{H2O}/g_{IOF}. The protein solubility had a different trend compared to water solubility—heat treatment and high-speed homogenization did not increase it (Fig. 2b). Heat is known to denature proteins and cause a reduction in their solubility. Only high-pressure homogenization considerably increased the protein solubility by more than 4 fold. The pH of the dispersion also was critical in protein solubilization during high-pressure homogenization. Indeed, protein solubility was higher at pH 7 than at pH 4.5 (Fig. 2b).

It is known that the solubility, swelling capacity, and water holding capacity of insoluble fibers can be considerably improved using high shear forces, like those generated with a microfluidizer (Hu et al. 2015; Mert et al. 2014; Wang et al. 2012, 2013). In our case, the increase in total water solubility, water holding capacity, and the protein solubility of IOF can be due to a combination of particle size reduction and increase in surface area. The formation of micropores in the particles due to the rapid change in pressure during high-pressure homogenization has been reported (Wang et al. 2013). In addition, high-pressure homogenization could break the cell wall of brans which improved the extractability of proteins as well as polysaccharides (Dong et al. 2011; Partanen et al. 2016). Differently, Sankaran et al. (2015) have reported an increase in particle size when combining enzymatic hydrolysis and microfluidization of carrot cell wall suspension, which was due to expansion of the particles after both treatments.

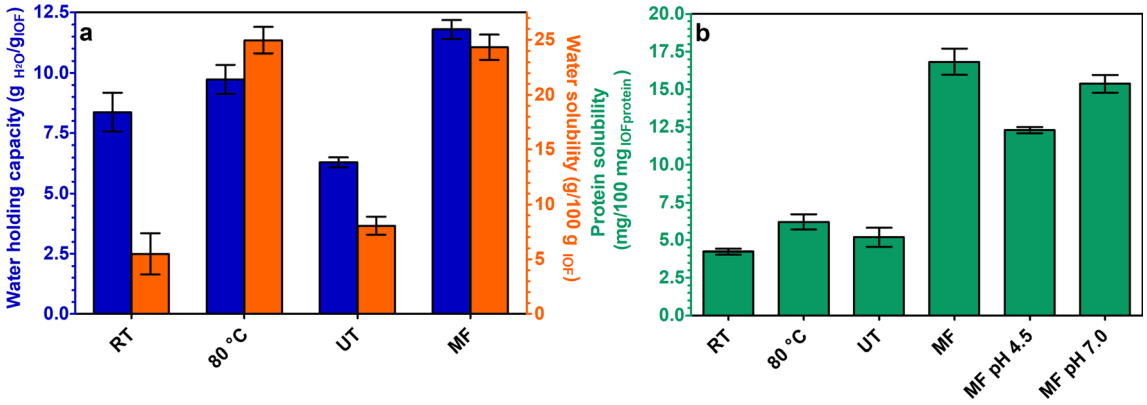

Fig. 2 (**a**) Water holding capacity (WHC, blue) and water solubility (orange) of insoluble oat fraction (IOF) after different treatments. (**b**) Protein solubility of insoluble oat fraction (IOF) after treatments. RT means room temperature; 80 °C means heated at 80 °C for 2h; UT means Ultra-Turrax, i.e., high-speed homogenization; MF means microfluidization, i.e., high-pressure homogenization. UT and MF were carried out at room temperature. Samples in MF at pH 4.5 and 7.0 were prepared by dispersing IOF in sodium citrate-phosphate buffer prior to MF treatment

We then studied the viscosity and physical stability of IOF and SOF dispersions (Table 2). The physical stability of the dispersions was followed using the Turbiscan stability index (TSI), which is a dimensionless parameter based on the changes of backscattered light over the sample prior to measurement. It is a convenient calibration-free method for studying sedimentation and aggregation phenomena as described by Bhattarai et al. (2020).

In general, 1% IOF dispersions underwent gravitational sedimentation for both thermal treatment at 80 °C for 2 h and high-speed homogenization (UT) due to its low viscosity (Table 2). Only by using high-pressure homogenization (MF), IOF dispersion showed a substantial increase in viscosity from 5 mPa·s to 46 mPa·s, which led to a more stable system. High disruptive shear forces are needed to increase IOF water solubility, protein solubility, and to reduce the size of insoluble particles. Soluble material contributed to the increase of viscosity by intermolecular entanglement, while insoluble materials could increase the volume fraction or crowding by swelling, which provide high resistance to flow (Hu et al. 2015; Wang et al. 2012, 2013). Leite et al. (2016) have shown a slight viscosity reduction after high-pressure homogenization for orange juice which was attributed to the degradation of pectin. Indeed, the impact of high-pressure homogenization

Table 2 Viscosity and TSI of IOF and SOF dispersions (at shear rate 10 s^{-1}) after thermal and/or mechanical treatments. UT is Ultra-Turrax; MF is microfluidization. Results represent mean ± standard deviation. TSI means Turbiscan stability index

Sample	Concentration (%)	Treatment	Viscosity @ 10 s^{-1} (mPa·s)	TSI	
				7 days	14 days
IOF	1%	80 °C, 2h	5.0 ± 0.4^{a} (supernatant)	32.9	37.0
		UT	5.3 ± 0.2^{a} (supernatant)	16.8	24.8
		MF	45.7 ± 2.2^{d}	0.1	0.1
		UT+MF	38.5 ± 3.1^{cd}	0.1	0.2
		MF+MF	33.6 ± 0.8^{c}	0.2	0.2
		MF+80 °C	14.5 ± 2.7^{b}	29.7	51.4
		MF (buffer pH 4.5)	46.0 ± 3.3^{d}	0.1	0.2
		MF (buffer pH 7.0)	43.4 ± 1.0^{cd}	0.2	0.2
	0.2%	MF	5.0 ± 0.2^{a}	21.2	30.8
		+0.5% SOF	80.4 ± 0.6^{e}	1.5	3.2
		+0.8% SOF	689.2 ± 1.8^{g}	0.3	0.7
SOF	0.5%	80 °C, 2h	76.2 ± 2.1^{e}	n.d.	n.d.
	1%	80 °C, 2h	843.0 ± 19.4^{g}	n.d.	n.d.
		80 °C, 2h + UT	164.2 ± 8.3^{f}	n.d.	n.d.
		80 °C, 2h, UT+MF	12.7 ± 1.7^{b}	n.d.	n.d.

$^{a, b, c, d, e, f, g}$: means with different letters in the same column are significantly different ($p < 0.05$). Note: n.d. means not determined. TSI for SOF was not measured since all SOF solutions were stable

on viscosity is dependent on the ratio of soluble and insoluble fiber, concentration, and extensity of the treatment. Extra treatments (UT+MF, MF+MF, and MF+80 °C) led to a reduction in viscosity. Only in the case of MF coupled with thermal treatment, however, did the viscosity reduce drastically leading to an unstable system. The application of high-pressure homogenization on diluted IOF dispersions did not allow a stable system. The stability was improved by adding viscous SOF solution to IOF suspension after homogenization.

On the other hand, SOF was highly soluble in water after thermal treatment at 80 °C for 2 h and formed stable solutions. 1% SOF solution had a viscosity highly dependent on the treatment applied. High shear forces led to a significant reduction of the viscosity (Table 2). This is likely due to the molecular degradation of the β-glucan polymeric chains as discussed by Kivelä et al. (2010).

Selected samples (IOF) were then further characterized to understand their sedimentation kinetics. We selected thermal treatment, UT, and combination of UT with MF (UT+MF). The first method is commonly employed for solubilization of β-glucan (Mäkelä et al. 2017), while UT and UT+MF were selected to understand possible changes induced to IOF. UT and MF are among the most commonly used methods for emulsion preparation, thus, were employed here to prepare IOF-stabilized emulsions (McClements 2016).

Figure 3a shows the evolution over time of the Turbiscan stability index (TSI) for 1% IOF in water after different processing conditions and macroscopic images of relevant suspensions after two weeks of storage at room temperature. We used IOF suspended in water without any treatment as a reference. As shown in Fig. 3 and in accordance with Table 2, the stability of the suspensions proceeded with increasing intensity of the treatment in the order: untreated (RT) < UT < UT+MF. The extent of the mechanical treatment was quantified by fitting the data with a one-phase exponential association model (Eq. 1, Data Analysis paragraph). Solid lines show the fitting with a 95% confidence interval represented by dashed lines. The inset in the figure shows the results of the fitting. UT treatment reduced 6-fold the rate of sedimentation of IOF suspension during storage compared to untreated sample (RT), however, over the long period, the sedimented layer of the two samples was similar (TSI_{max} and Fig. 3b). On the other hand, microfluidization was able to further reduce the rate of sedimentation leading to a homogeneous system that was stable for more than a month (low TSI_{max} and Fig. 3b). This can be due to the increased viscosity of the microfluidized IOF suspension compared to the UT-treated one (Table 2). The disruptive mechanical forces during homogenization increased the fraction of the solubilized material (Fig. 2a) and increased the water-holding capacity (Fig. 2a) by either decreasing the particle size or increasing the exposure of a more hydrophilic site to water (Wang et al. 2012, 2013). Therefore, regarding using IOF to form emulsions, the combination of UT+MF seems the most promising method to obtain a homogeneous dispersion which can possibly lead to stable emulsions.

We then determined ζ-potential and surface-tension reduction (difference between surface tension of solvent and surface tension of solvent with oat fraction) with the aim to determine the possible emulsifying abilities of IOF and SOF.

In general, the ζ-potential of both IOF and SOF was negative, independent of the dispersion method used. SOF had a ζ-potential of around -1.0 mV after solubilization at 80 °C for 2 h in water or buffer. The independence of ζ-potential value from the buffer confirms that this fraction had a low number of charged molecules in the solution. On the other hand, IOF ζ-potential was highly dependent on the treatment and pH value of the buffer (Fig. 4). Thermal treatment and homogenization increased the absolute value of ζ-potential while the buffer at

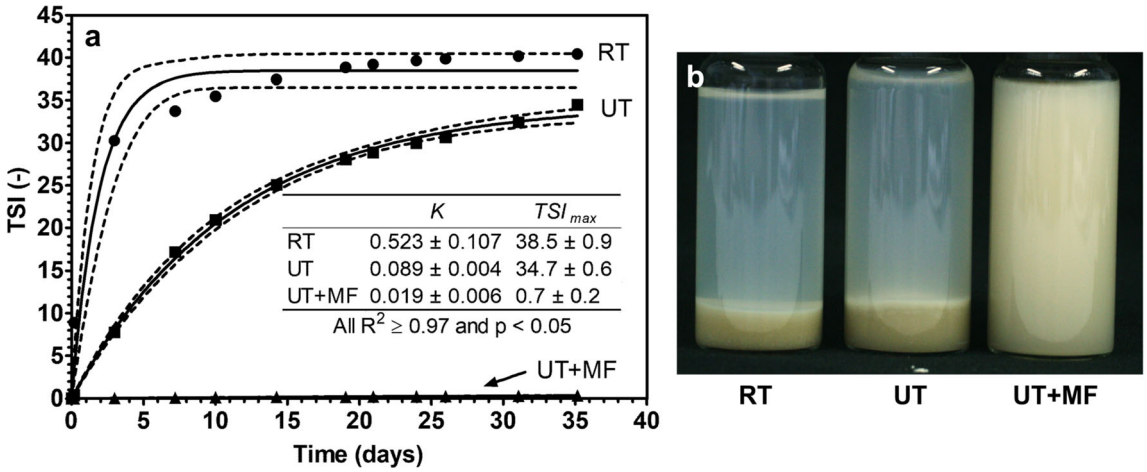

Fig. 3 (**a**) Turbiscan stability index (TSI) as a function of time during storage at room temperature of suspensions containing 1% insoluble oat fraction (IOF) after mixing with water at room temperature (RT), treatment with high-speed homogenizer (Ultra-Turrax, UT), and a combination of high-speed homogenization and high-pressure homogenization (Ultra-Turrax + Microfluidizer, UT+MF). (**b**) Macroscopic appearance of the samples described in (**a**) after two weeks of storage at room temperature

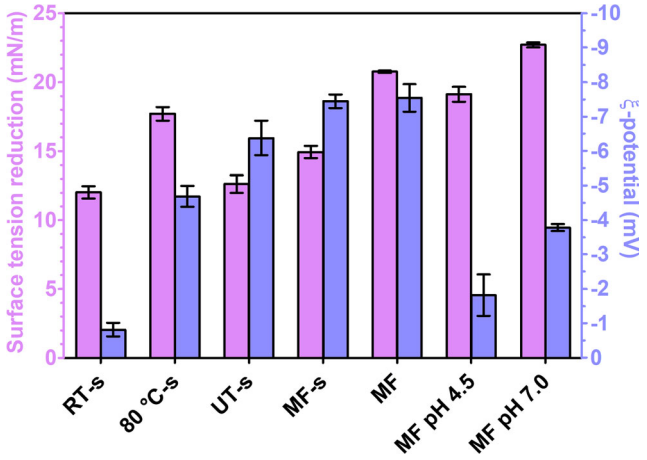

Fig. 4 Reduction of surface tension and ζ-potential of insoluble oat fraction (IOF) suspensions after different treatments. RT means room temperature; 80 °C means heated at 80 °C for 2h; UT means Ultra-Turrax that is high-speed homogenization; MF means microfluidization that is high-pressure homogenization. UT and MF were carried out at room temperature. Samples in MF at pH 4.5 and 7.0 were prepared by dispersing IOF in sodium citrate-phosphate buffer prior to MF treatment. The letter "s" means supernatant after mild centrifugation

different pH values reduced it drastically. The presence of ions in the buffer could have electrostatically shielded the charges present in IOF (*cf.* MF with MF pH 4.5 and MF pH 7.0, Fig. 4). The differences in ζ-potential with the two pH values tested can be attributed to the ionization of proteins which at low pH can be closer to their isoelectric point and thus have less charged groups on the molecules. However, even if IOF ζ-potential was affected by treatment and medium, with its absolute value below 30 mV, IOF does not guarantee electrostatic stabilization of oil droplet in emulsions (Mikkonen et al. 2016b).

The reduction of surface tension of SOF in water after thermal treatment was 4.2 ± 0.5 mN/m compared to distilled water. The low amount and solubility of protein (Table 1), coupled with the impurities of this fraction (low amount of phenols and phytic acid and high concentration of hemicelluloses), did not allow a substantial reduction of the surface tension, which in turn can have a negative impact on emulsion formation and stabilization. Conversely, IOF showed a surface tension reduction between 12 and 23 mN/m, which was dependent on the treatment and pH value of the buffer (Fig. 4). Already by mixing IOF with water at room temperature a certain reduction of the surface tension in the resulting supernatant was observed, probably because soluble amphiphilic molecules, such as proteins and saponins present in oat bran, were able to dissolve (Laine et al. 2011; Ralla et al. 2018). The surface tension reduction observed in IOF was lower than that of oat-bran extract rich in saponins (Ralla et al. 2018), but it is similar to that of hemicelluloses extracted from softwood rich in galactoglucomannans and residual lignin (Valoppi et al. 2019a). Thermal treatment and high-pressure homogenization in water and buffer gave the highest surface tension reduction values. Interestingly, the supernatant of IOF after high-pressure homogenization (MF-s, Fig. 4) showed lower values compared to the IOF suspension after the same treatment (MF, Fig. 4). Therefore, the particles suspended in the sample had a certain surface activity, meaning they could have bound to the surface molecules, such as phenolic compounds, similarly to the case we reported previously on hemicelluloses extracted from softwood (Lahtinen et al. 2019; Valoppi et al. 2019a). The maximum reduction of the surface tension was achieved by dispersing IOF in the buffer at pH 7 before MF treatment. Free fatty acids and proteins can most probably be ionized at this pH value, increasing the overall interfacial activity of IOF. We also found that surface-tension–reduction results showed a positive significant correlation with protein solubility results ($r = 0.90$, $p < 0.05$), indicating that proteins in the aqueous phase mostly contribute to surface tension reduction.

Emulsions

To evaluate the ability of IOF and SOF suspensions as emulsifiers, we prepared emulsions with oil content between 0.5 and 5% (w/w). The suspensions were obtained by mixing 0.2–1% (w/w) IOF and SOF with water or buffer followed by magnetic stirring at 80 °C for 2 h; an additional IOF-containing aqueous phase was obtained using high-pressure homogenization (microfluidizer).

In general, both suspensions were able to form emulsions with no visible oil floating on top of the container soon after homogenization. This was expected for IOF due to its ability in reducing the surface tension and its composition (Table 1), though, surprisingly also SOF was able to form emulsions. During storage, however, flocculation occurred in emulsions to a different extent. Figure 5 shows the emulsions after two weeks of storage at room temperature obtained using IOF and SOF suspensions, as well as selected micrographs.

All emulsions obtained with SOF had a fast flocculation regardless of oil and SOF concentration or processing conditions. White aggregates floated on top of the container after homogenization and during storage as shown in Fig. 5a. The aggregates were composed of oil droplets surrounded by a bright area as revealed by fluorescence microscopy after Calcofluor staining (Fig. 5b). Due to the composition of SOF (Table 1), bright areas can be β-glucan molecules that accumulated at the oil/water interface. Even though SOF showed a low ability to reduce surface tension, during emulsion formation, proteins (around 11%, Table 1) and β-glucan (77.5%, Table 1) were able to stabilize the interface. It is known that β-glucan can form hydrophobic cavities in triple-helix conformation that can trap guest molecules (Sletmoen and Stokke 2008), similar to cyclodextrins (Astray et al. 2009) and amylose (Putseys et al. 2010). Therefore, triacylglycerol molecules could be trapped in β-glucan helices, anchoring β-glucan at the oil/water interface

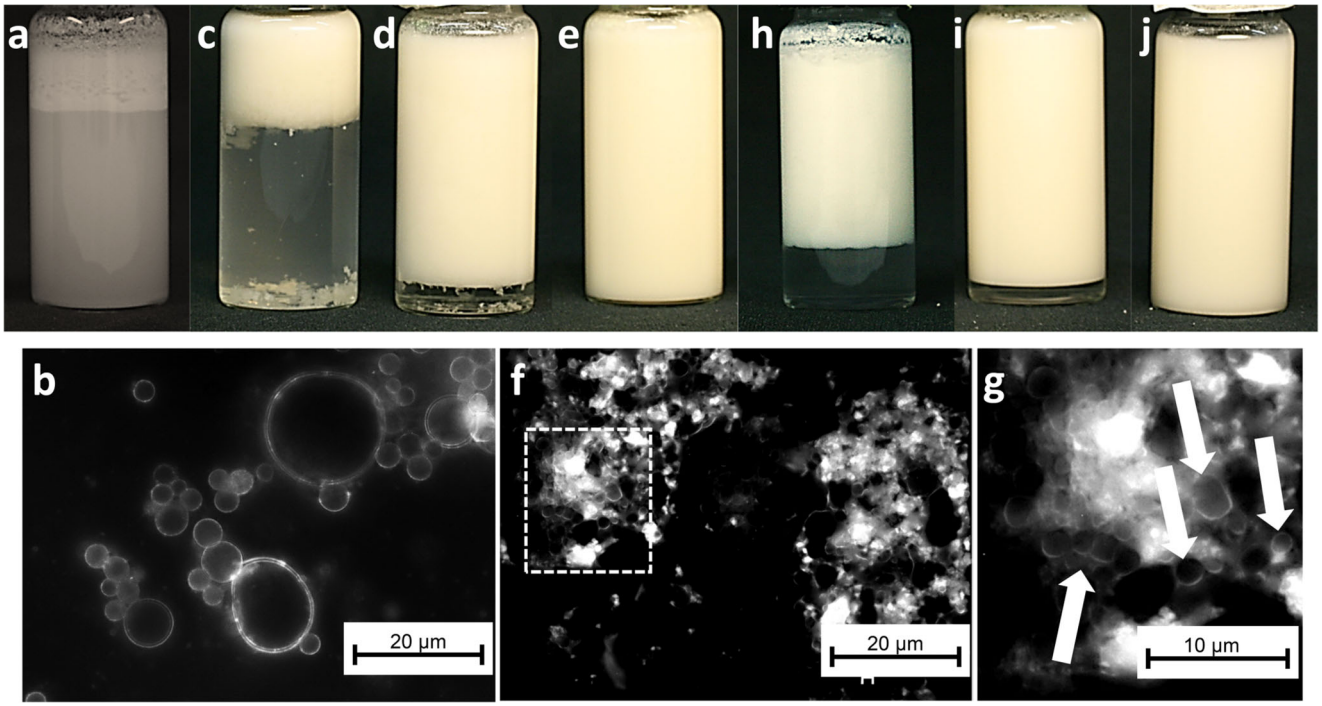

Fig. 5 Emulsions prepared with oat soluble fraction (SOF) and different concentrations of oat insoluble fraction (IOF) and oil and selected micrographs. Pictures taken after 2 weeks of storage at room temperature. Emulsions were prepared by homogenization with Ultra-Turrax followed by microfluidizer. (**a**) 1% SOF and 2.5% oil with (**b**) fluorescent microscopy image of the top creamed layer after Calcofluor staining, (**c**) 0.2% IOF and 0.5% oil, (**d**) 0.5% IOF and 1.25% oil, (**e**) 1% IOF and 2.5% oil with (**f**) relevant fluorescent microscopy image after Calcofluor staining and (**g**) magnification of the highlighted area in (**f**) with arrows showing some oil droplets, (**h**) 1% IOF and 5% oil, (**i**) 1% IOF undergone to microfluidization before emulsion preparation (MF-IOF) and 2.5% oil, and (**j**) 0.5% IOF + 2.5% oil added with 0.5% SOF after emulsion preparation. Scale bars are 20 μm in (**b**) and (**f**) and 10 μm in (**g**)

as observed in fluorescence microscopy. It is also known that β-glucan has a natural tendency to aggregate over time (Li et al. 2011), which in our case seems to be boosted by the presence of oil-forming macroscopic-aggregates after homogenization. However, further studies are needed to elucidate the mechanism behind the interfacial activity of β-glucan and its hydrophobically driven aggregation.

Regarding IOF, the emulsions obtained with this fraction had a storage stability that was dependent on IOF and oil concentrations and processing conditions. At low concentrations of IOF and oil (Fig. 5c), the emulsion underwent phase separation. A creamed layer on top is separated from a clear serum layer on the bottom. By keeping the surfactant-to-oil-ratio (SOR) constant to 0.4 and increasing both IOF and oil, the serum layer decreased, eventually disappearing as shown in Fig. 5e. The reduction of the serum layer with increasing concentration of oil and IOF was probably due to the increasing amount of soluble proteins and volume fraction of fibers added to the emulsion coupled with the homogenization process. Zhu et al. (2017) have shown that high-pressure treatment significantly improved solubility, emulsifying, and foaming capacity of rice bran proteins. Insoluble fibers, after homogenization, can considerably improve their swelling capacity and hold more water and oil compared to their native form (Wang et al. 2012, 2013). The stable emulsion was composed of particles with oil droplets attached on their surface (Fig. 5f, g). In this case, oil droplets were also surrounded by bright areas which can be accumulations of β-glucan and arabinoxylan (21% and 25% of IOF, respectively, Table 1). Fluorescence in particles could also be due to insoluble β-glucan and arabinoxylan in the material. The emulsions formed with IOF were much more stable than those obtained with SOF. To gain more insight on the mechanism behind emulsion formation and stabilization using IOF, we prepared emulsions using the supernatant after centrifuging the MF-treated IOF, and the resulting emulsion was unstable (data not shown). This clearly indicates the fundamental role of the insoluble particles on emulsion formation and stabilization. Therefore, oil droplets after formation were anchored on the surface of the insoluble particles (Fig. 5g) leading to stable emulsions. Another interesting point is that we were only able to obtain stable emulsions with stable suspensions. Therefore, we hypothesized that there might be two mechanisms involved in emulsion stabilization with IOF. The first regards oil droplet formation, while the second is the anchoring of the oil droplets to the surface of insoluble particles. The

oil surface can be stabilized due to (i) the higher protein content in IOF (almost 22%, Table 1) and increase in protein solubility after homogenization (Fig. 2b), (ii) the presence of saponins which are small molecular-weight naturally occurring surfactants (Ralla et al. 2018), (iii) the presence of β-glucan which could have helped droplet interface stabilization as previously discussed, and (iv) arabinoxylan, which being insoluble can stabilize the interface via Pickering stabilization as shown for emulsions stabilized with beech and birch xylans (Mikkonen 2020) and/or due to the phenolic compounds attached to arabinoxylans, the latter can be anchored at the interface similar to galactoglucomannans extracted from softwood (Lehtonen et al. 2018). After oil droplet formation, the droplets were anchored and retained on the particle surface. This can be due to the exposure of sites with, e.g., bound proteins on the particle surface able to anchor the droplets. Oil droplets are adsorbed on the surface of the particles, the latter being orders of magnitude bigger than oil droplets; therefore, to obtain stable emulsions it is necessary to first obtain stable suspensions. There might be an equilibrium between the oil droplets with the tendency for creaming and the insoluble particles with the tendency for sedimenting. This unique mechanism gives IOF stabilized emulsions a high storage stability. However, we observed that reducing the SOR (by increasing oil content) or homogenizing IOF suspension before emulsion preparation led again to the formation of unstable emulsions (Fig. 5h, i). The inability to retain water by the emulsion can be due to the limited amount of soluble proteins and the saturation of the available particle surfaces for the increased amount of oil. An excessive homogenization process can degrade the particle size and volume fraction, as well as the polymeric chains as shown for β-glucan (Kivelä et al. 2010). The addition of 0.5% SOF to the unstable IOF-containing emulsions led again to stable emulsions over time (Fig. 5j), which is most probably because SOF was able to hold extra water and increase the viscosity of the emulsion, kinetically stabilizing the system (McClements 2016), However, if the SOR was low, the addition of SOF could not substantially improve the emulsion's storage stability. We demonstrated that SOF is not suitable to undergo mechanical treatments that can degrade β-glucan molecules, and it forms aggregates with oil, but it is effective in stabilizing an emulsion after homogenization. Finally, the stability of the IOF emulsion was affected by pH. Indeed, emulsion stabilized with IOF (1% IOF and 2.5% oil) at pH 4.5 was not as stable as the emulsions at pH 7 (data not shown), which correlates to the trend of protein solubility and surface tension.

To better understand the effect of processing conditions and pH on emulsions formed with IOF, we analyzed the particle size distribution of selected aqueous phases and the corresponding emulsions (Table 3).

In general, all homogenized IOF suspensions had 90% of the particles smaller than 100 μm. Double homogenization or change in pH led to a further reduction of the particle dimensions as shown by D[3,2], D[4,3], and distribution percentiles. However, the reduction led to a broader distribution as shown by the increase of SPAN. The emulsions obtained with corresponding IOF suspensions had bigger particle dimeters (e.g., *cf.* IOF+MF suspension with IOF emulsion or IOF+MF+MF suspension with IOF+MF emulsion). It has to be remembered that both oil droplets and IOF particles are simultaneously detected during size measurement. Therefore, the increase in particle diameter in emulsions can be due to the oil attached to the surface of the particles or possible aggregation induced by oil. Moreover, the energy delivered to the system during homogenization is constant. This mechanical energy is used for both particle size reduction and formation of small oil droplets. Thus, the presence of oil reduces the energy delivered to the particles compared to neat suspensions, possibly contributing to the observed size increase.

It can be concluded, however, that an excessive increase in particle diameter after emulsion formation is responsible for the formation of the serum layer during storage. Bigger particles tend to flocculate and cream faster, as described by the Stokes' law (McClements 2016).

We demonstrated that side streams from oat production can be used as novel bio-based emulsifiers and stabilizers without any further chemical derivatization or fractionation. In most cases, the extraction of the surface-active fraction from side streams is performed before emulsion preparation (Laine et al. 2011; Ralla et al. 2017, 2018). Extracts can be further fractionated or purified using chemical (antisolvent precipitation) and physical (centrifugation) methods to increase the performance of emulsifiers extracted from side streams (Bhattarai et al. 2019; Valoppi et al. 2019a). However, even if in most of the cases extraction is carried out using water and food-grade solvents, an abundant part of the starting material is discharged. This makes sense in materials that are inedible by themselves, but that contain edible molecules, such as wood (Mikkonen 2020). In the case of fully edible materials, like in the case of bran, the extraction of emulsifiers can further generate waste material. Our approach was to avoid any extraction/manipulation of oat side streams and use them to obtain stable suspensions and emulsions. This has the advantage to increase the value of the side stream which enters back into the food production chain, in perfect respect of the circular economy model. The complex mixture of the insoluble oat fraction can form stable emulsions that can be used as ingredients to produce functional foods or can be directly consumed as functional foods, such as oat-based beverages after appropriate formulation modification (Valoppi et al. 2019b). In addition, the soluble fraction from oat production side

Table 3 The particle size of IOF suspensions and corresponding emulsions. For emulsion preparation, native IOF suspension was mixed with oil and homogenized by Ultra-Turrax (UT) and microfluidizer (MF), except one sample (IOF+MF) in which the IOF suspension was treated with microfluidizer before emulsion preparation. The final emulsion contained 1% IOF and 2.5% oil. Results represent mean ± standard deviation

Sample type	Sample name	D [3,2] (μm)	D [4,3] (μm)	Dv(10) (μm)	Dv(50) (μm)	Dv(90) (μm)	SPAN (-)
Suspension	IOF+MF	23.0 ± 1.0^{c}	54 ± 2^{cd}	11.9 ± 0.7^{bc}	48 ± 1^{c}	103 ± 3^{bc}	1.9
	IOF+MF+MF	4.3 ± 0.1^{a}	31 ± 2^{a}	3.1 ± 0.1^{a}	21 ± 1^{a}	70 ± 6^{a}	3.2
	IOF+MF (pH 4.5)	16.0 ± 0.4^{b}	36 ± 1^{ab}	7.7 ± 0.3^{ab}	28 ± 1^{ab}	75 ± 5^{a}	2.4
	IOF+MF (pH 7.0)	17.0 ± 0.6^{b}	45 ± 3^{bc}	10.0 ± 2^{bc}	37 ± 4^{b}	93 ± 0^{ab}	2.2
Emulsion (1% IOF + 2.5% oil) (UT+MF)	IOF	38.0 ± 1.0^{e}	62 ± 1^{d}	18.3 ± 0.4^{d}	53 ± 2^{c}	119 ± 0^{cd}	1.9
	IOF+MF	29.5 ± 0.1^{d}	50 ± 2^{c}	14.6 ± 0.3^{cd}	37 ± 0^{b}	104 ± 7^{bc}	2.4
	IOF (pH 4.5)	5.6 ± 0.5^{a}	80 ± 5^{e}	10.0 ± 1.0^{bc}	74 ± 5^{d}	150 ± 10^{e}	1.9
	IOF (pH 7.0)	57.0 ± 2.0^{f}	84 ± 4^{e}	36.0 ± 2.0^{e}	80 ± 3^{d}	139 ± 6^{de}	1.3

$^{a, b, c, d, e, f}$: means with different letters in the same column are significantly different ($p < 0.05$)

streams can be used as a thickening agent to improve emulsion stability where the amount of insoluble fraction is not enough to guarantee a prolonged physical stability of the system.

Conclusions

Stable suspension and emulsion could be formed by insoluble oat fractions (IOF) after high-pressure homogenization. This is due to the increase in protein solubility and reduction in surface tension and particle size. The phase stability is dependent on the IOF concentration, the ratio of IOF to oil, and the intensity of the homogenization. The emulsion formed by IOF was different than traditional emulsions where the oil droplets are formed and suspended in continuous phase. With IOF emulsion, the oil droplets were anchored on the surface of the suspended particles. Therefore, emulsion stability was largely dependent on the stability of the suspension. The soluble oat fraction (SOF) formed a viscous solution after heat treatment; however, it degraded by high-pressure homogenization and formed aggregates with lipids in emulsion. Therefore, the best use of SOF was to increase the viscosity and improve the stability of IOF suspension or emulsion after homogenization. Both materials were nutritious with soluble and insoluble fibers, proteins, and phytochemicals, and we proved they have well-performed technical functionality with no further fractionation and/or chemical derivatization.

Acknowledgments We thank Christian Malmberg for fruitful discussion on the manuscript and Julia J. Varis for drawing the graphical abstract.

Author Contribution F.V.: methodology, preliminary analysis, data curation, writing—original draft, and writing—review and editing. Y.W.: methodology, investigation, formal analysis, data curation, and writing—review and editing. G.A.: methodology, preliminary analysis, and review and editing. L.J.P.: resources and review and editing. K.S.M.: conceptualization, funding acquisition, resources, project administration, supervision, and review and editing.

Funding Open access funding provided by University of Helsinki including Helsinki University Central Hospital. Lantmännen Research Foundation (Stockholm, Sweden) is acknowledged for funding (grant number 2017H020) and providing the SOF and IOF samples.

Declarations

Conflict of Interest The authors declare no conflict of interest.

References

Ahmad, A., Anjum, F. M., Zahoor, T., Nawaz, H., & Ahmed, Z. (2010). Extraction and characterization of beta-d-glucan from oat for industrial utilization. *International Journal of Biological Macromolecules, 46*(3), 304–309.

Ahmad, M., Zaffar, G., Dar, Z. A., & Habib, M. (2014). A review on oat (avena sativa l.) as a dual-purpose crop. *Scientific Research and Essays, 9*(4), 52–59.

Anal, A. K. (2017). Food processing by-products and their utilization: introduction. In A. K. Anal (Ed.), *Food processing by-products and their utilization* (pp. 1–10). Hoboken: Wiley.

Arvanitoyannis, I. S., & Tserkezou, P. (2008). Wheat, barley and oat waste: a comparative and critical presentation of methods and potential uses of treated waste. *International Journal of Food Science and Technology, 43*(4), 694–725.

Astray, G., Gonzalez-Barreiro, C., Mejuto, J. C., Rial-Otero, R., & Simal-Gandara, J. (2009). A review on the use of cyclodextrins in foods. *Food Hydrocolloids, 23*(7), 1631–1640.

Bhattarai, M., Pitkänen, L., Kitunen, V., Korpinen, R., Ilvesniemi, H., Kilpeläinen, P. O., et al. (2019). Functionality of spruce galactoglucomannans in oil-in-water emulsions. *Food Hydrocolloids, 86*, 154–161.

Bhattarai, M., Valoppi, F., Hirvonen, S.-P., Hietala, S., Kilpeläinen, P., Aseyev, V., et al. (2020). Time-dependent self-association of spruce galactoglucomannans depends on ph and mechanical shearing. *Food Hydrocolloids, 102*, 105607.

Bhatty, R. S. (1993). Physicochemical properties of roller-milled barley bran and flour. *Cereal Chemistry, 70*, 397–402.

Călinoiu, L. F., Cătoi, A.-F., & Vodnar, D. C. (2019). Solid-state yeast fermented wheat and oat bran as a route for delivery of antioxidants. *Antioxidants, 8*(9), 372.

Charalampopoulos, D., Wang, R., Pandiella, S. S., & Webb, C. (2002). Application of cereals and cereal components in functional foods: a review. *International Journal of Food Microbiology, 79*(1-2), 131–141.

Dong, X., Zhao, M., Shi, J., Yang, B., Li, J., Luo, D., Jiang, G., & Jiang, Y. (2011). Effects of combined high-pressure homogenization and enzymatic treatment on extraction yield, hydrolysis and function properties of peanut proteins. *Innovative Food Science & Emerging Technologies, 12*(4), 478–483.

El-Din, F. B. A. M., Ahmed, Z. S., Latief, A. R. A., El-Akel, A. T., & Abou-Raya, S. H. (2009). Chemical, physical, nutritional, and sensory properties of high fiber healthy corn snacks. *Food, 3*(1), 53–57.

Englyst, H. N., Quigley, M. E., & Hudson, G. J. (1994). Determination of dietary fibre as non-starch polysaccharides with gas-liquid chromatographic, high-performance liquid chromatographic or spectrophotometric measurement of constituent sugars. *Analyst, 119*(7), 1497–1509.

Faix, O. (1991). Classification of lignins from different botanical origins by ft-ir spectroscopy. *Holzforschung - International Journal of the Biology, Chemistry, Physics and Technology of Wood, 45*(s1), 21.

Floch, J., Lees, M., & Sloane-Stanley, G. H. (1957). A simple method for the isolation and purification of total lipides from animal tissues. *Journal of Biological Chemistry, 226*, 497–509.

Fritsch, C., Staebler, A., Happel, A., Marquez, M. A. C., Aguilo-Aguayo, I., Abadias, M., et al. (2017). Processing, valorization and application of bio-waste derived compounds from potato, tomato, olive and cereals: a review. *Sustainability, 9*(8), 1492.

Gangopadhyay, N., Hossain, M. B., Rai, D. K., & Brunton, N. P. (2015). A review of extraction and analysis of bioactives in oat and barley and scope for use of novel food processing technologies. *Molecules, 20*(6), 10884–10909.

Grundy, M. M. L., McClements, D. J., Ballance, S., & Wilde, P. J. (2018). Influence of oat components on lipid digestion using an in vitro model: impact of viscosity and depletion flocculation mechanism. *Food Hydrocolloids, 83*, 253–264.

Helkar, P. B., Sahoo, A. K., & Patil, N. J. (2016). Review: food industry by-products used as a functional food ingredients. *International Journal of Waste Resources, 6*(3), 1000248.

Hu, R., Zhang, M., Adhikari, B., & Liu, Y. (2015). Effect of homogenization and ultrasonication on the physical properties of insoluble wheat bran fibres. *International Agrophysics, 29*(4), 423–432.

Isikgor, F. H., & Becer, C. R. (2015). Lignocellulosic biomass: a sustainable platform for the production of bio-based chemicals and polymers. *Polymer Chemistry, 6*(25), 4497–4559.

Izydorczyk, M. S., McMillan, T., Bazin, S., Kletke, J., Dushnicky, L., Dexter, J., Chepurna, A., & Rossnagel, B. (2014). Milling of canadian oats and barley for functional food ingredients: oat bran and barley fibre-rich fractions. *Canadian Journal of Plant Science, 94*(3), 573–586.

Kamal-Eldin, A., Laerke, H. N., Knudsen, K. E., Lampi, A. M., Piironen, V., Adlercreutz, H., et al. (2009). Physical, microscopic and chemical characterisation of industrial rye and wheat brans from the nordic countries. *Food & Nutrition Research, 53*. https://doi.org/10.3402/fnr.v3453i3400.1912.

Kapreliants, L., & Zhurlova, O. (2017). Technology of wheat and rye bran biotransformation into functional ingredients. *International Food Research Journal, 24*(5), 1975–1979.

Kivelä, R., Pitkänen, L., Laine, P., Aseyev, V., & Sontag-Strohm, T. (2010). Influence of homogenisation on the solution properties of oat β-glucan. *Food Hydrocolloids, 24*(6-7), 611–618.

Lahtinen, M. H., Valoppi, F., Juntti, V., Heikkinen, S., Kilpeläinen, P. O., Maina, N. H., et al. (2019). Lignin-rich phwe hemicellulose extracts responsible for extended emulsion stabilization. *Frontiers in Chemistry, 7*, 871.

Laine, P., Toppinen, E., Kivelä, R., Taavitsainen, V.-M., Knuutila, O., Sontag-Strohm, T., Jouppila, K., & Loponen, J. (2011). Emulsion preparation with modified oat bran: optimization of the emulsification process for microencapsulation purposes. *Journal of Food Engineering, 104*(4), 538–547.

Lehtonen, M., Teräslahti, S., Xu, C., Yadav, M. P., Lampi, A.-M., & Mikkonen, K. S. (2016). Spruce galactoglucomannans inhibit lipid oxidation in rapeseed oil-in-water emulsions. *Food Hydrocolloids, 58*(Supplement C), 255–266.

Lehtonen, M., Merinen, M., Kilpeläinen, P. O., Xu, C., Willför, S. M., & Mikkonen, K. S. (2018). Phenolic residues in spruce galactoglucomannans improve stabilization of oil-in-water emulsions. *Journal of Colloid and Interface Science, 512*(Supplement C), 536–547.

Leite, T. S., Augusto, P. E. D., & Cristianini, M. (2016). Frozen concentrated orange juice (fcoj) processed by the high pressure homogenization (hph) technology: effect on the ready-to-drink juice. *Food and Bioprocess Technology, 9*(6), 1070–1078.

Li, W., Cui, S. W., Wang, Q., & Yada, R. Y. (2011). Studies of aggregation behaviours of cereal β-glucans in dilute aqueous solutions by light scattering: Part i. Structure effects. *Food Hydrocolloids, 25*(2), 189–195.

Luhaloo, M., Mårtensson, A. C., Andersson, R., & Åman, P. (1998). Compositional analysis and viscosity measurements of commercial oat brans. *Journal of the Science of Food and Agriculture, 76*(1), 142–148.

Luithui, Y., Baghya Nisha, R., & Meera, M. S. (2019). Cereal by-products as an important functional ingredient: effect of processing. *Journal of Food Science and Technology, 56*(1), 1–11.

Lv, D., Chen, F., Yin, L., & Liu, C. (2019). Emulsifying properties of wheat bran arabinoxylan modified with whey protein isolate using the Maillard reaction. *Journal of Dispersion Science and Technology, 41*(14), 2082–2090.

Maes, C., & Delcour, J. A. (2002). Structural characterisation of water-extractable and water-unextractable arabinoxylans in wheat bran. *Journal of Cereal Science, 35*(3), 315–326.

Mäkelä, N., Maina, N. H., Vikgren, P., & Sontag-Strohm, T. (2017). Gelation of cereal β-glucan at low concentrations. *Food Hydrocolloids, 73*, 60–66.

McClements, D. J. (2016). *Food emulsions: principles, practices, and techniques*. Boca Raton: CRC Press.

Mert, B., Tekin, A., Demirkesen, I., & Kocak, G. (2014). Production of microfluidized wheat bran fibers and evaluation as an ingredient in reduced flour bakery product. *Food and Bioprocess Technology, 7*(10), 2889–2901.

Mikkonen, K. S. (2020). Strategies for structuring diverse emulsion systems by using wood lignocellulose-derived stabilizers. *Green Chemistry, 22*(4), 1019–1037.

Mikkonen, K. S., Merger, D., Kilpeläinen, P., Murtomaki, L., Schmidt, U. S., & Wilhelm, M. (2016a). Determination of physical emulsion

stabilization mechanisms of wood hemicelluloses via rheological and interfacial characterization. *Soft Matter, 12*(42), 8690–8700.

Mikkonen, K. S., Xu, C., Berton-Carabin, C., & Schroën, K. (2016b). Spruce galactoglucomannans in rapeseed oil-in-water emulsions: efficient stabilization performance and structural partitioning. *Food Hydrocolloids, 52*, 615–624.

Morales-Ortega, A., Carvajal-Millan, E., Lopez-Franco, Y., Rascon-Chu, A., Lizardi-Mendoza, J., Torres-Chavez, P., et al. (2013). Characterization of water extractable arabinoxylans from a spring wheat flour: rheological properties and microstructure. *Molecules, 18*(7), 8417–8428.

Onipe, O. O., Jideani, A. I. O., & Beswa, D. (2015). Composition and functionality of wheat bran and its application in some cereal food products. *International Journal of Food Science and Technology, 50*(12), 2509–2518.

Papageorgiou, M., Lakhdara, N., Lazaridou, A., Biliaderis, C. G., & Izydorczyk, M. S. (2005). Water extractable (1→3,1→4)-β-d-glucans from barley and oats: an intervarietal study on their structural features and rheological behaviour. *Journal of Cereal Science, 42*(2), 213–224.

Partanen, R., Sibakov, J., Rommi, K., Hakala, T., Holopainen-Mantila, U., Lahtinen, P., et al. (2016). Dispersion stability of non-refined turnip rapeseed (brassica rapa) protein concentrate: impact of thermal, mechanical and enzymatic treatments. *Food and Bioproducts Processing, 99*, 29–37.

Patel, S. (2015). Cereal bran fortified-functional foods for obesity and diabetes management: triumphs, hurdles and possibilities. *Journal of Functional Foods, 14*, 255–269.

Putseys, J. A., Lamberts, L., & Delcour, J. A. (2010). Amylose-inclusion complexes: formation, identity and physico-chemical properties. *Journal of Cereal Science, 51*(3), 238–247.

Ralla, T., Salminen, H., Edelmann, M., Dawid, C., Hofmann, T., & Weiss, J. (2017). Sugar beet extract (beta vulgaris l.) as a new natural emulsifier: emulsion formation. *Journal of Agricultural and Food Chemistry, 65*(20), 4153–4160.

Ralla, T., Salminen, H., Edelmann, M., Dawid, C., Hofmann, T., & Weiss, J. (2018). Oat bran extract (Avena sativa L.) from food by-product streams as new natural emulsifier. *Food Hydrocolloids, 81,* 253–262.

Robertson, J. A., & Eastwood, M. A. (1981). An examination of factors which may affect the water holding capacity of dietary fibre. *British Journal of Nutrition, 45*, 83–88.

Saeed, F., Pasha, I., Anjum, F. M., Sultan, J. I., & Arshad, M. (2014). Arabinoxylan and arabinogalactan content in different spring wheats. *International Journal of Food Properties, 17*(4), 713–721.

Sankaran, A. K., Nijsse, J., Bialek, L., Bouwens, L., Hendrickx, M. E., & Van Loey, A. M. (2015). Effect of enzyme homogenization on the physical properties of carrot cell wall suspensions. *Food and Bioprocess Technology, 8*(6), 1377–1385.

Satue, M. T., Huang, S. W., & Frankel, E. N. (1995). Effect of natural antioxidants in virgin olive oil on oxidative stability of refined, bleached, and deodorized olive oil. *Journal of the American Oil Chemists' Society, 72*(10), 1131–1137.

Schlemmer, U., Frølich, W., Prieto, R. M., & Grases, F. (2009). Phytate in foods and significance for humans: food sources, intake, processing, bioavailability, protective role and analysis. *Molecular Nutrition & Food Research, 53*(S2), S330–S375.

Sharma, S. K., Bansal, S., Mangal, M., Dixit, A. K., Gupta, R. K., & Mangal, A. K. (2016). Utilization of food processing by-products as dietary, functional, and novel fiber: a review. *Critical Reviews in Food Science and Nutrition, 56*(10), 1647–1661.

Sletmoen, M., & Stokke, B. T. (2008). Higher order structure of (1,3)-beta-d-glucans and its influence on their biological activities and complexation abilities. *Biopolymers, 89*(4), 310–321.

Song, X., & Hubbe, M. (2014). Cationization of oat β-d glucan as a dry-strength additive for paper. *Tappi Journal, 13*(7), 57–64.

Soycan, G., Schar, M. Y., Kristek, A., Boberska, J., Alsharif, S. N. S., Corona, G., et al. (2019). Composition and content of phenolic acids and avenanthramides in commercial oat products: are oats an important polyphenol source for consumers? *Food Chemistry: X, 3*, 100047.

Stevenson, L., Phillips, F., O'Sullivan, K., & Walton, J. (2012). Wheat bran: its composition and benefits to health, a european perspective. *International Journal of Food Sciences and Nutrition, 63*(8), 1001–1013.

Stewart, D., & McDougall, G. (2014). Oat agriculture, cultivation and breeding targets: implications for human nutrition and health. *British Journal of Nutrition, 112*(S2), S50–S57.

Sun, L. H., Lv, S. W., Chen, C. H., & Wang, C. (2019). Preparation and characterization of rice bran protein-stabilized emulsion by using ultrasound homogenization. *Cereal Chemistry, 96*(3), 478–486.

Synytsya, A., & Novak, M. (2014). Structural analysis of glucans. *Annals of Translational Medicine, 2*(2), 17.

Valoppi, F., Lahtinen, M. H., Bhattarai, M., Kirjoranta, S. J., Juntti, V. K., Peltonen, L. J., Kilpeläinen, P. O., & Mikkonen, K. S. (2019a). Centrifugal fractionation of softwood extracts improves the biorefinery workflow and yields functional emulsifiers. *Green Chemistry, 21*(17), 4691–4705.

Valoppi, F., Maina, N., Allén, M., Miglioli, R., Kilpeläinen, P. O., & Mikkonen, K. S. (2019b). Spruce galactoglucomannan-stabilized emulsions as essential fatty acid delivery systems for functionalized drinkable yogurt and oat-based beverage. *European Food Research and Technology, 245*(7), 1387–1398.

Wang, T., Sun, X., Zhou, Z., & Chen, G. (2012). Effects of microfluidization process on physicochemical properties of wheat bran. *Food Research International, 48*(2), 742–747.

Wang, T., Sun, X., Raddatz, J., & Chen, G. (2013). Effects of microfluidization on microstructure and physicochemical properties of corn bran. *Journal of Cereal Science, 58*(2), 355–361.

Wang, Y.-J., Yang, L., & Sontag-Strohm, T. (2020). Co-migration of phytate with cereal β-glucan and its role in starch hydrolysis in-vitro. *Journal of Cereal Science, 93*, 102933.

Yamazaki, E., Murakami, K., & Kurita, O. (2005). Easy preparation of dietary fiber with the high water-holding capacity from food sources. *Plant Foods for Human Nutrition, 60*(1), 17–23.

Zang, X. D., Yue, C. H., Wang, Y. X., Shao, M. L., & Yu, G. P. (2019). Effect of limited enzymatic hydrolysis on the structure and emulsifying properties of rice bran protein. *Journal of Cereal Science, 85*, 168–174.

Zhu, S. M., Lin, S. L., Ramaswamy, H. S., Yu, Y., & Zhang, Q. T. (2017). Enhancement of functional properties of rice bran proteins by high pressure treatment and their correlation with surface hydrophobicity. *Food and Bioprocess Technology, 10*(2), 317–327.